Robotic Fabrication of Shear Timber Connections: Exploring the Structural Behavior of Robotically Fabricated Mechanical and Adhesive Shear Connections in Timber Structures

Bindels T.H.W. (t.h.w.bindels@student.tue.nl / 0944588)
Eindhoven University of Technology

***Abstract*—The construction industry faces significant challenges across multiple aspects, including, but not limited to, productivity, costs, demand, and sustainability. To address these challenges, the industry must innovate rapidly to adapt to current demands. One approach to achieving this is by increasing digitization and automation within the industry. While sectors such as manufacturing adopted automated workflows long ago, the construction industry still lags behind. Recent developments indicate gradual progress, such as the growing use of prefabricated elements, which offer numerous advantages over traditional construction methods. This research delves into the prefabrication possibilities within the construction industry, specifically focusing on the robotic fabrication of structural elements. It concentrates on the robotic fabrication of timber trusses using either mechanical fasteners or adhesives, both of which are highly suitable for integration into a robotic workflow. By doing so, this thesis contributes to the advancement of knowledge on robotic applications in the construction industry.**

***Index Terms*—robotic fabrication, automation, fastener, adhesive, connection, timber, digital design, computational design**

I. Introduction

A. Motivation

MANY of the problems in the AEC industry can be linked to two main themes: productivity and sustainability. Productivity is particularly critical as demand continues to increase while the industry's productivity fails to keep pace. Robotic processes offer a significant improvement by enabling continuous, off-site fabrication of building parts. These processes are not affected by weather conditions or the availability of skilled labor. Moreover, on-site assembly of these prefabricated elements requires fewer laborers and is much quicker.

Robotic fabrication also has the potential to reduce environmental impact by using materials more efficiently and minimizing waste. When digital design processes are aimed at robotic fabrication, waste can be further reduced through smart assembly and patterning algorithms. Additionally, processes can easily adapt to new building materials, including biobased options.

Timber is a particularly suitable material for sustainable use, provided it is sourced properly. Timber is well-suited for robotic processes, as it does not require drying or layering like 3D printing materials, nor does it involve complex and energy-intensive processes like 3D steel printing. The primary drawback is that robotic fabrication with timber tends to be subtractive, necessitating careful design and detailing to minimize waste.

B. State of the Art

Research on robotic applications within the built environment is rapidly evolving and there is a wide range of research that touches upon this topic. In structural applications that use timber as a building material, several notable research projects stand out. One prominent example is the DFAB HOUSE, shown in fig. 1a, which is a collaboration of multiple ETH Zurich chairs and faculties as well as industrial partners [1]. The DFAB HOUSE is designed, planned, and (mostly) fabricated using digital processes. One of the processes utilized, is the assembly of the spatial modules, of which one is shown in fig. 1b [2]. This robotic process is both digitally planned and executed using multiple robotic techniques. It ensures the precise placement

of structural members and incorporates additional tools for fastening and assembly. These tools include sawing, in-place milling, and a tracking system, all integrated into the robotic workflow.

(a) DFAB HOUSE

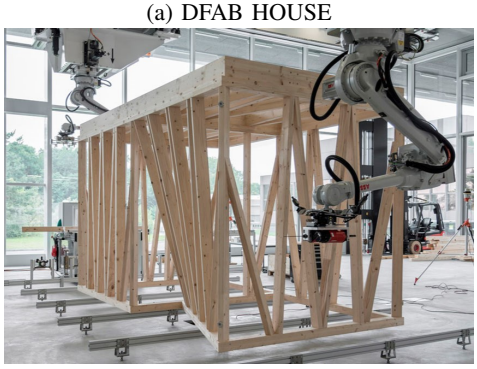

(b) Spatial structure

Fig. 1: Finished DFAB house and spatial structure [1].

Another notable example that utilizes adhesive is the BUGA Wood Pavilion by the University of Stuttgart [3]. This project requires a complex digital design and assembly sequence to ensure all the cassettes fit together properly. The fabrication of these cassettes involves multiple tasks, including picking and placing the elements, adhesive dispensing, nail fastening, and milling. Since adhesive connections are subject to strict building code regulations, the adhesive dispensing process had to undergo thorough testing with numerous parameter studies.

Last, another project of ETH Zurich is referenced: The roof structure of the university's digital fabrication lab, where the DFAB spatial structures mentioned earlier are fabricated. These trusses are parametrically designed and robotically fabricated in collaboration with industry partners [4]. The trusses have multiple lap joints fastened using mechanical fasteners. Placement algorithms for the fasteners were crucial to avoid collisions while ensuring sufficient strength.

(a) BUGA Wood Pavilion

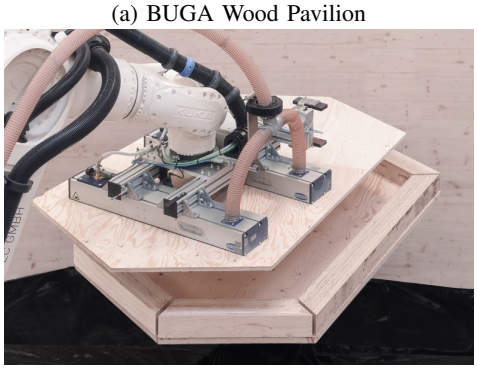

(b) Fabrication

Fig. 2: Finished BUGA Wood Pavilion and the fabrication process of the timber cassettes [3].

(a) Arch_Tec_Lab roof

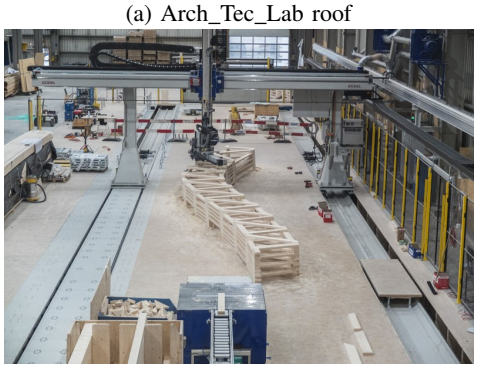

(b) Fabrication

Fig. 3: Arch_Tec_Lab timber roof trusses [4].

C. Contribution of this Proposal

This research aims to develop a robotic fabrication process that is capable of fabricating timber trusses either glued or mechanically fastened. By doing so, it provides a process that can fabricate structural members suitable for load-bearing applications in an automatic process. It builds upon previous research, of which examples are shown in section I-B, by combining the various robotic processes, joining methods, and structural elements it adds to existing literature. To achieve this, the following research question must be answered:

"How Do Adhesive and Mechanical Shear Timber Connections Perform Structurally When Fabricated Using a Robotic Process?"

To answer this research question, the following sub-questions must be answered:

- How can adhesive or mechanical shear joints be optimized during the design phase?
- What are the different parameters of an adhesive dispensing system, and how are these controlled to ensure reliable dispensing of the adhesive?
- Which subsystems are required to ensure proper curing of the adhesive joint?
- How can an individual adhesive dispensing system be integrated in a robotic workflow?
- What strength and reliability can be achieved in an adhesive timber joint fabricated by a robotic process?

To answer the set research objectives, the following steps are taken. First, a design toolbox using Grasshopper is developed. This toolbox quickly assesses and analyzes mechanical joints in a truss configuration, allowing the study of different parameters' effects on strength. Additionally, the toolbox serves as a general tool for designers to experiment with or optimize specific design scenarios. Next, a robotic setup is developed in the structural engineering lab to fabricate such a truss physically. This setup includes various existing tools, adapted tools, and newly developed tools that must be integrated to function as a cohesive system. The robotically fabricated elements are then tested in shear to evaluate any differences between the proposed robotic process and traditional fabrication methods. All these results are gathered to: First, assess whether the proposed robotic setup can fabricate equally strong connections as traditional methods. Second, assess different design options and their various parameters, and how they affect the structural performance.

This paper starts by providing important background information on mechanical and adhesive shear connections in section II respectively. These sections cover general information about the available connections, stress and/or strength calculations, and design considerations. Second, in section III the used approaches are elaborated. Third, the results gathered using these methods are presented in section IV. The findings are discussed in section V, after which recommendations for further research are given in section VI. Last, the thesis concludes in section VII.

II. Literature Review

A. Mechanical Fasteners

Dowel-type joints in timber structures loaded in shear can fail in multiple ways. This is first presented by [5], which describes three distinct failure modes I to III. These failure modes are based on the number of plastic hinges developing in the fastener: I

1) No plastic hinges develop, only embedment of the timber.
2) One plastic hinges develops.
3) Two plastic hinges develop.

Important to recognize is that these failure modes have a different level of safety. Embedment of the timber is considered a brittle failure mode, whereas failure of the dowel with two plastic hinges is considered a plastic mode. In the design of the connections it is important to consider the desired ductility.

The basis of the design rules given by EN 1995-1-1 is based on this theory, with some small adjustments. Within this theory, failure depends on the two important parameters discussed before: Timber embedment strength and fastener yield moment. In case the timber members are of a different species or one of the members is loaded at an angle to the grain, the embedment strengths are related by

$$\beta = \frac{f_{\mathrm{h,2,k}}}{f_{\mathrm{h,1,k}}} \tag{1}$$

As a convention, for single lap joints the subscript "1" refers to the thinnest member, whereas "2"

refers to the thicker member. In case of double lap joints, “1” refers to the outer members whereas “2” refers to the inner member. For double lap joints it is assumed that the outer members are of equal thickness. This model is also referred to as the European yield model (EYM). The failure modes in EN 1995-1-1 are shown in fig. 4. In the upcoming sections the equations for single lap joints are dervied, the procedure to derive the ones for double lap joints is similar.

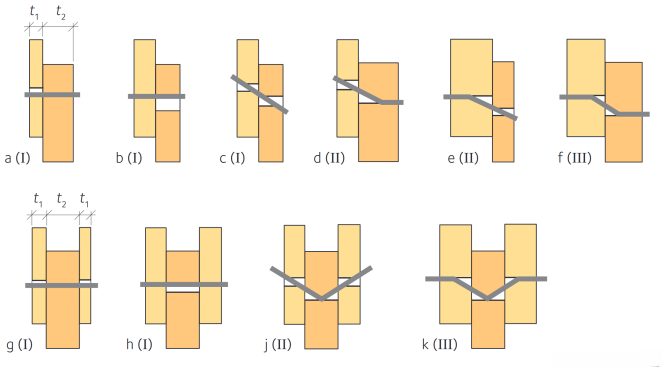

Fig. 4: EYM failure modes included in EN 1995-1-1 [6].

In EN 1995-1-1, the shear resistances of the connections shown in fig. 4 realized using dowel-type fasteners are calculated by the equations shown in figs. 5 and 6.

It can be seen that the equations show close resemblance to the solutions derived in analytically, as they are based on them. However, the following differences can be observed:

- There are additional constants introduced.
- In certain equations an additional term including $F_{\mathrm{ax,Rk}}$ is introduced.

The constants are a result of the combination of timber and steel. Safety factors of these materials differ, as well as additional factors such as k_{mod}, taking into account moisture contents for timber. However, the moisture content is not relevant for the yield moment of the fastener. Consequently, these additional constants are introduced to counter the negative effects of k_{mod} and γ_{M} on the yield moment of the fastener [8]. The term including $F_{\mathrm{ax,Rk}}$ is a direct result of the so-called rope effect. This effect occurs when a fastener is deformed such that it becomes loaded (partially) in tension, as shown in fig. 7. This provides additional resistance for the connection. [8] derived the inclusion of the rope effect analytically, from this a friction

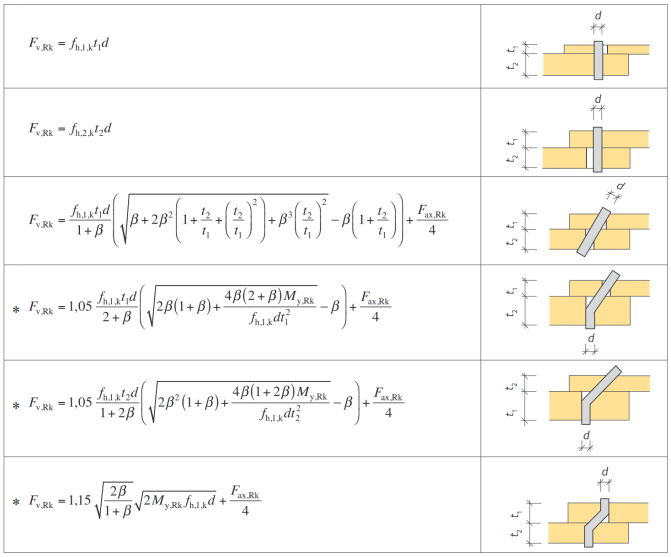

Fig. 5: EN 1995-1-1 shear resistances for single shear [6].

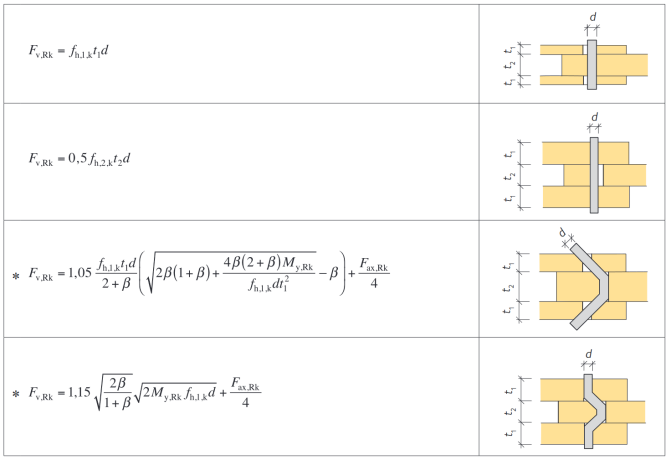

Fig. 6: EN 1995-1-1 shear resistances for double shear [6].

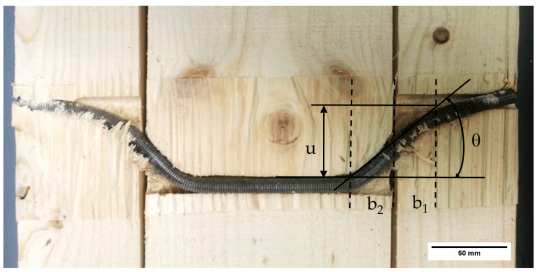

Fig. 7: Rope effect due to large deformations causing additional tensile forces [7].

coefficient μ resulted. In EN 1995-1-1, this is set at $\mu = 0.25$, resulting in the $\frac{1}{4}$. Moreover, there are limits specified to how much rope effect may be added. For screws, this is 100% of the other term, causing it to double at most. However, for dowels no contribution of the rope effect may be added.

For groups of fasteners, [9] has researched how the force distribution is over the fasteners. It has been revealed that it is not evenly distributed due to imperfections of the timber and fastener placement. In reality, the first and last fastener receives the highest load. This behavior is schematized in fig. 8. Consequently, the shear resistance of the entire joint is not simply the multiplication of all the fasteners. This effect is especially relevant for larger-diameter fasteners, as these behave mostly linear elastic. Fasteners with a smaller diameter often allow for plasticity, and in turn enables redistribution of the forces. To take the group effect into account, a so-called effective number of fasteners n_{ef} is included in EN 1995-1-1, which can be calculated using.

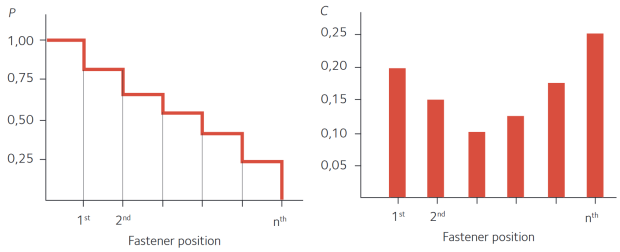

(a) Force along timber member. (b) Force distribution over fasteners.

Fig. 8: Group effect fastener behavior [6].

B. Adhesive Connections

Timber adhesive connections can be categorized into various groups, as classified in fig. 9. Hybrid wood joints use adhesives to connect different materials, often steel to timber. Well-known examples include glued-in rods or plates. Wood-to-wood joints can be further distinguished into continuous or local joints. Continuous joints are found in built-up elements or products such as CLT and glulam. Local joints transfer forces at specific points and include examples such as lap joints, glued-on gusset plates, and finger joints.

Mechanical fasteners can provide ductility, which results in failure mechanisms that show sufficient warning before failure. In contrast, adhesive joints do not exhibit this feature. While there are slight differences in the elasticity of adhesives, their failure modes are generally brittle, which is a concern for structural engineering applications. The different links that can fail in a lap joint are shown in fig. 10. Each of the links in the connection fails differently, of which the various failure types are

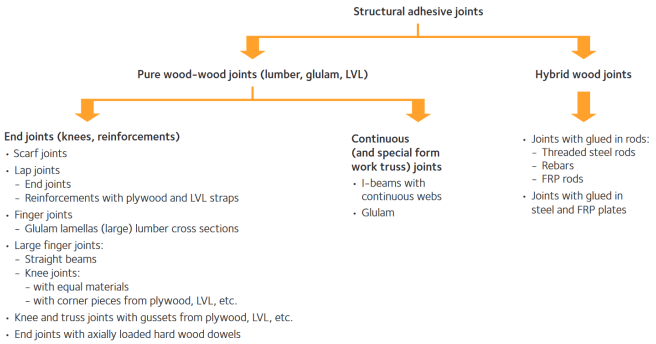

Fig. 9: Different categories of adhesive joints [6].

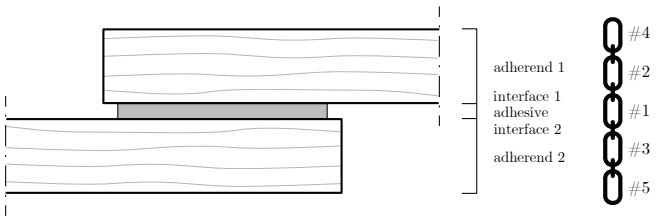

Fig. 10: Different links that can fail in an adhesive timber connection.

shown in fig. 11. These can be described as follows:

- **Adhesion failure:** The interface between the adhesive and timber fails.
- **Cohesion failure:** The adhesive itself fails.
- **Adhesion/cohesion failure:** A combination of the two failure modes.
- **Adherend failure:** Failure of the timber itself.

The failure modes in which the adhesive (or part of it) fails are all brittle and occur very suddenly. Among these failure modes, the least brittle is the failure of the timber. Nevertheless, this still constitutes a very brittle failure mode. The failure of the timber becomes increasingly concerning when the lap joint is angled, causing one of the timber members to be loaded partially perpendicular to the grain.

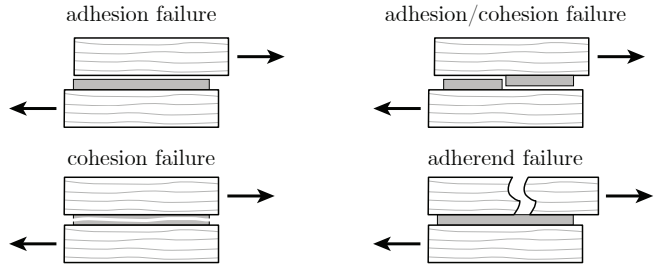

Fig. 11: Different types of failure that can occur in an adhesive connection.

Closed-form adhesive stress solutions are compared using the case study shown in fig. 12. The Hart-Smith analysis uses an adhesive plastic stress of $\tau_{\mathrm{p}} = 3\,\mathrm{N/mm^2}$. In fig. 13, the shear

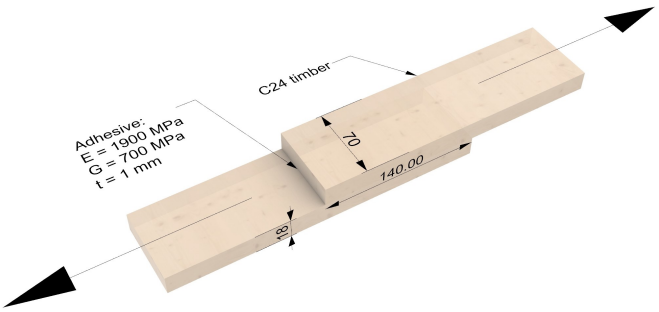

Fig. 12: SLJ case study and its parameters.

stresses along the adhesive bond are shown. It shows clear stress peaks near the ends of the joint, whereas shear stresses are almost negligible in the middle of the joint. These shear stress peaks at the ends of the joint are not realistic, as in reality, the shear stress should drop to zero since there is no material to shear against. Other analytical solutions have addressed this phenomenon. It can be seen that the theories generally agree. Goland and Reissner, Ojalvo and Eidinoff, and Hart-Smith differ only slightly. Hart-Smith's model shows an early cutoff near the ends due to the plasticity that is taken into account. Volkersen's theory predicts slightly lower stresses near the ends but higher stresses toward the middle compared to the other theories.

The peel stresses for the case study are shown in fig. 14. Volkersen's theory is evidently absent, as it does not account for the peel stresses caused by the bending of the joint. The other three theories almost perfectly agree for this case study. The peel stresses are relatively high near the joint ends and quickly decrease. The peel stresses decrease to the point where a zone is in compression. Near the middle of the joint, the peel stresses become stable and almost zero. Once again, the stresses are almost negligible in the middle, indicating that increasing the bond length beyond a certain point is not beneficial.

The analytical results in figs. 13 and 14 are compared to the stresses extracted from the ABAQUS model in figs. 15 and 16. The shear stresses show an almost perfect agreement with the Goland and Reissner and Ojalvo and Eidinoff solution. The peel stresses also show nearly perfect

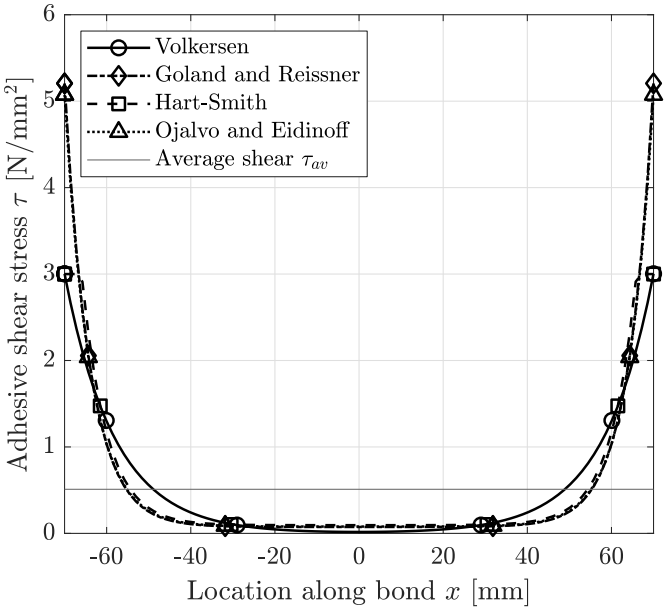

Fig. 13: Shear stress τ in adhesive along bond length.

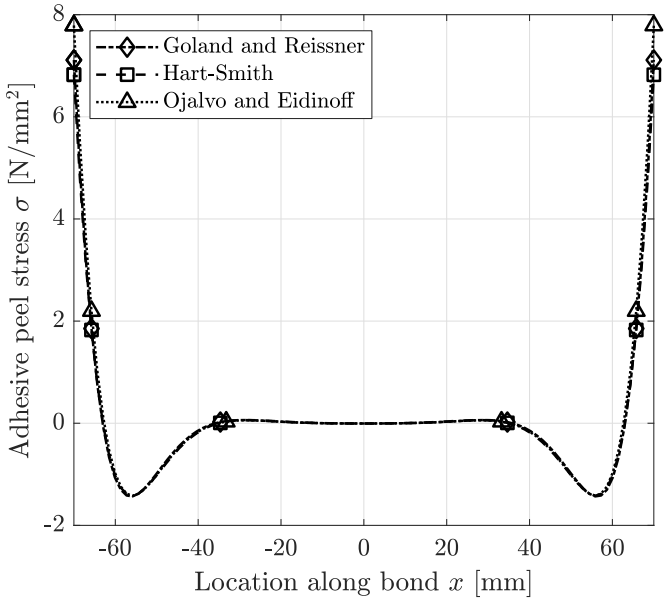

Fig. 14: Normal (peel) stress σ in adhesive along bond length.

agreement. There is a slight discrepancy where the peel stress drops in the compressive region. However, this can explained by the fact that the FEM model can be modeled much more accurately. For this purpose, it was a relatively crude model. However, with improvements to the meshing (including a finer mesh near stress peaks) and parameter tuning a more accurate stress analysis is expected.

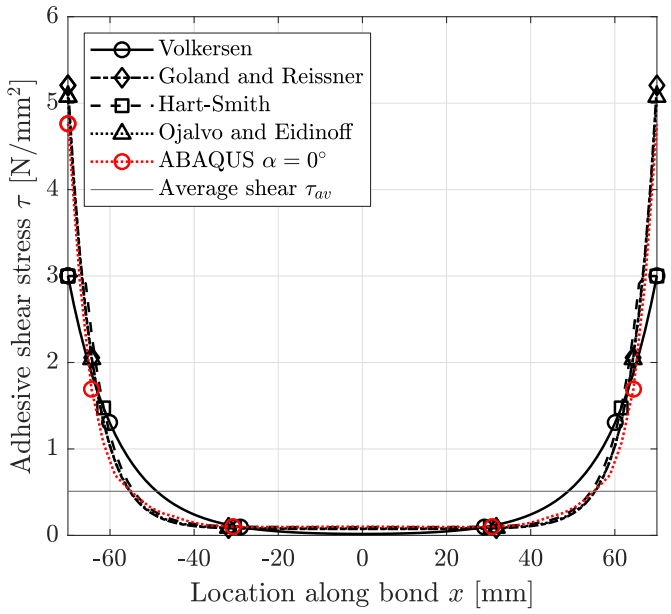

Fig. 15: Shear stress τ in adhesive along bond length.

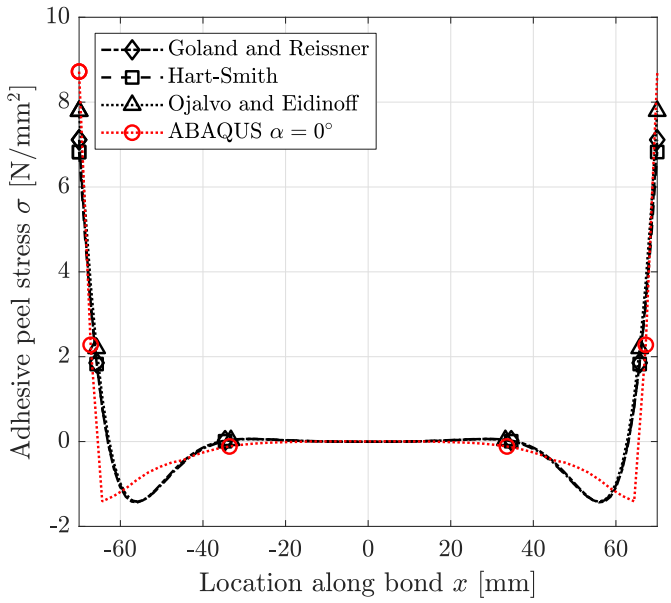

Fig. 16: Normal (peel) stress σ in adhesive along bond length.

III. Methodology

In the robotic setup in fig. 17 the following subsystems and locations can be distinguished:

1) Pickup location of the timber members, which are vertically stacked in order of placement.
2) IRB 1200 robot equipped with a parallel gripper responsible for pick-and-place actions.
3) The stationary drilling station for the AMB milling motor.
4) Pickup location of the screws.

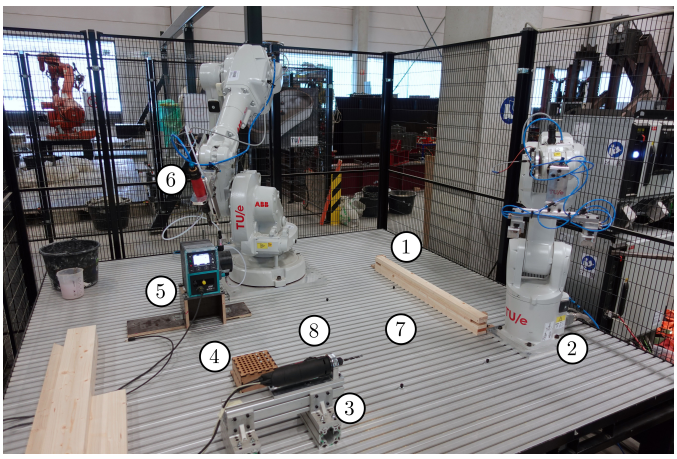

Fig. 17: The complete robotic setup to fabricate shear connections.

Fig. 18: Pickup location of the timber members.

5) Adhesive dispensing system using the Qdos peristaltic pump.
6) IRB 1600 robot that is responsible for all fastening tasks, with a dedicated end-effector for both gluing and screwing.
7) Work object location where the truss elements are fabricated.
8) Reorientation location where the members can be temporarily placed when the gripper needs to be relocated.

The pickup location of the timber members is shown in fig. 18. The members are stacked vertically in order of appearance. The MDF brackets are calibrated and ensure that the members are always aligned properly. The parallel gripper is shown in fig. 19, it consists of the following components:

1) MDF backstop blocks prevent the timber piece from being pushed too far in the gripper (e.g. when being drilled). The timber members are gripped so that there is 3 mm of free vertical space left.
2) The parallel gripper is spaced 240 mm apart. The brackets are aligned such that there is 4 mm of free horizontal space left.
3) The parallel gripper is operated pneumatically. The pneumatic system is connected via a relay, which can be controlled using a digital signal.

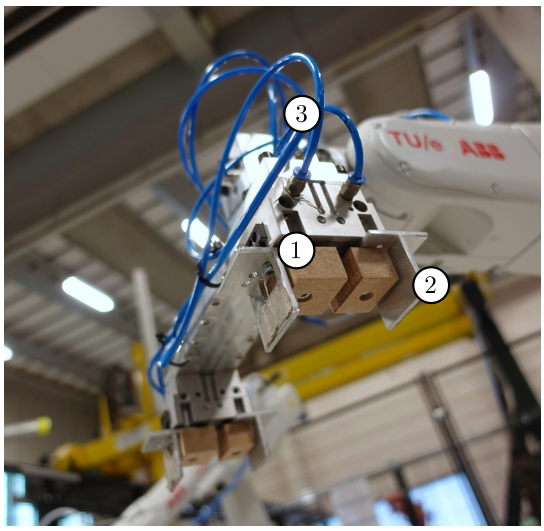

Fig. 19: Parallel gripper setup.

The amount of adhesive dispensed per area ρ_{a} is based on the system parameters, which must meet the requirements as specified by the adhesive supplier ρ_{req}. To control the dispensed adhesive, the parameters of the dispensing process shown in fig. 21 must be determined. This results in the following condition:

$$\rho_{\mathrm{req,min}} \leq \rho_{\mathrm{a}} = \frac{Q}{v\,s} \leq \rho_{\mathrm{req,max}} \tag{2}$$

where

ρ_{a}	is the adhesive per area [g/mm^2]
Q	system flow rate [g/s]
v	robot speed [mm/s]
s	adhesive spread [mm]
ρ_{req}	supplier requirements [g/mm^2]

Fig. 20: Adhesive dispensing subsystem.

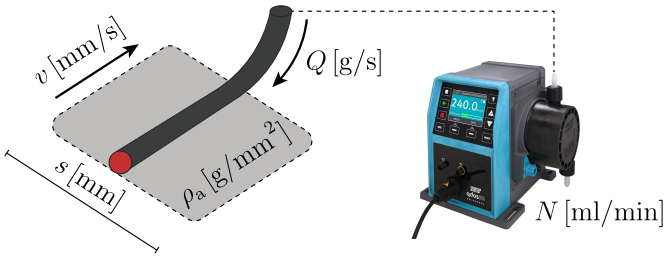

Fig. 21: The parameters of the adhesive dispensing process.

The end-effector used combines the dispensing nozzle and the screwdriver, and is shown in fig. 22. It consists of the following components:

1) Magnet bit holder suitable for large screws.
2) Pneumatically (7 bars) activated screwdriver that is operated at an RPM of 550 rev/min.
3) AC006 capacitive sensor with a range of 2 mm.
4) The sensor provides a digital input that is used to detect the final screwing distance and stops the screwing process.
5) The dispensing nozzle is located next to the screwdriver, and is located in height above the screwdriver and sensor.

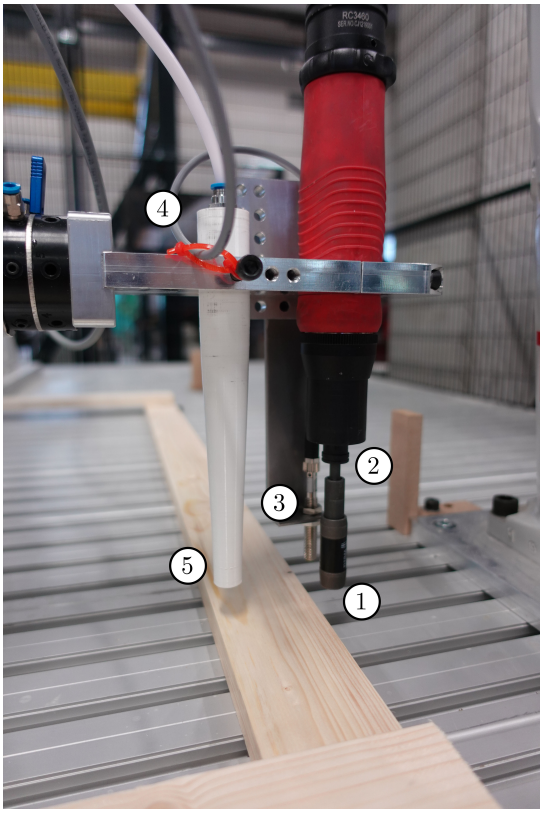

Fig. 22: Fastening end-effector with the screwdriver and the nozzle.

To assess the performance of the developed robotic fabrication process, various parameters of the robotic system are compared to a traditional fabrication method using adhesives. The experiment is based on a double lap joint loaded in shear, as shown in fig. 23. The adhesive dispensing pattern, screws to introduce clamping pressure, and a hybrid adhesive-screw connection are investigated.

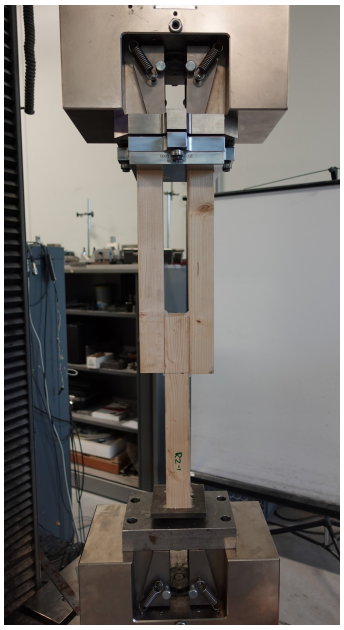

(a) Setup

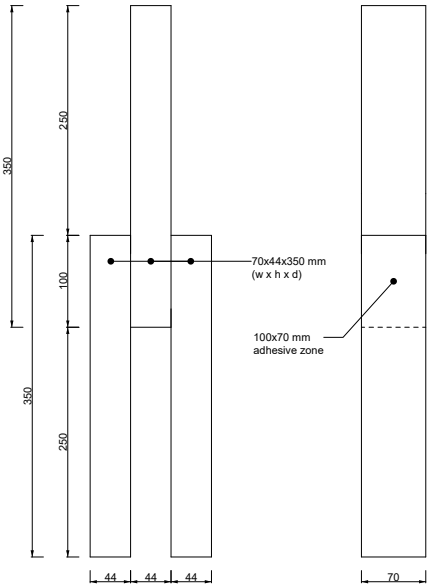

(b) Dimensions

Fig. 23: The experimental setup used and sample dimensions.

IV. Results

The robotic fabrication process fabricates discretized elements that can be combined to form a complete truss. One of the members is shown in fig. 25. During the fabrication process the following observations were made:

- Careful calibration of all end effectors, ancillary elements, and workpieces is required. Small deviations can quickly accumulate, resulting in discrepancies of a few millimeters.
- The drilling process requires the parallel gripper to hold the elements at their ends. This sometimes proved challenging for larger pieces due to their weight. For example, the 1 m members were gripped at one end, leaving the other 800 mm extended. On a few occasions, the member nearly fell out of the gripper due to its weight.
- Repositioning and turning the members to align them properly with the drill requires considerable time. The robot has to move relatively slowly to prevent vibrations from causing the member to shift or fall out of the gripper. Half of the fabrication time is attributed solely to predrilling the holes. Moreover, multiple repositioning steps increase the likelihood of errors and deviations in the final product.
- The current drill speed starts at an RPM of 3500 rev/min. However, operating the drill at higher speeds causes the relatively soft and low-density timber to burn.
- For these relatively small joints, it is crucial to carefully calibrate the adhesive dispensing timing. The start time of dispensing must be accurately timed to avoid moving too soon and thereby not dispensing adhesive on part of the joint.
- Screws must be chosen carefully to meet multiple criteria. One important criterion is ensuring that the bit magnet can easily snap to the screw head. For smaller heads, calibration and small discrepancies become more critical compared to larger heads.

In general, the robotic process required very little to no manual intervention. However, in one instance, a long member that needed to be predrilled was not properly gripped. Due to its weight, it partly fell out of the gripper and had to be repositioned manually.

Consequently, there was a slight discrepancy in the hole location. When the screw was inserted at this location, it did not pass through the predrilled hole but screwed directly into the timber. As a result, the members were not properly clamped together, leading to an insufficient bond.

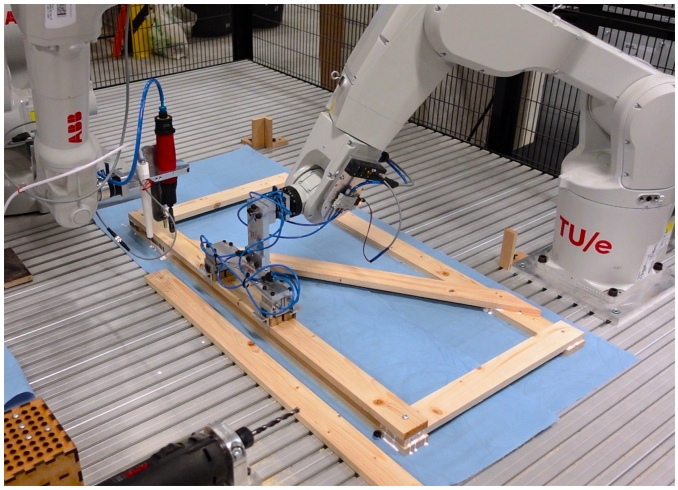

Fig. 24: Robotic fabrication process of a discrete element.

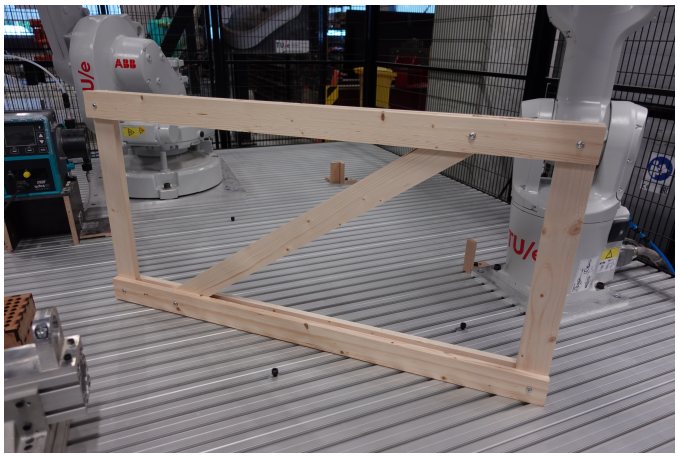

Fig. 25: One fabricated segment after the fully automated robotics fabrication process.

The results of the benchmark set are shown in fig. 26, it can be seen that the stiffness of the joint is very similar for all samples. The maximum vertical displacement only reaches about 1.75 mm. There is relatively little spread, and a relatively constant failure load. A 5% watered-down adhesive mixture is used for the pumping process, and the results are compared to the benchmark set in fig. 27. The joint stiffness is almost equal to the benchmark, and the maximum shear strength is roughly the same. Some

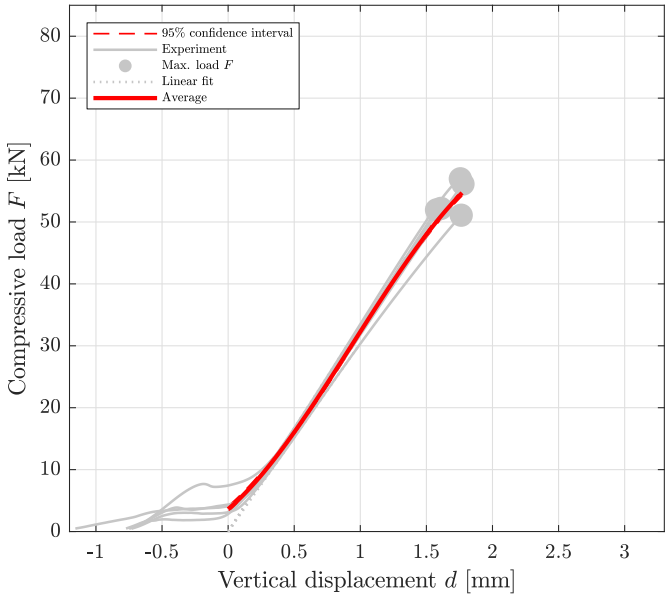

Fig. 26: Load-displacement results of the benchmark samples R1 (**red**).

samples reached slightly lower strengths, whereas one was significantly stronger.

The robotic fabrication process applies the adhesive using a nozzle and predetermined settings. The results of these samples are shown in fig. 28. Once again, the stiffness of the joint is almost equal to the benchmark set. Moreover, three of the samples reached significantly higher joint strengths, while only one performed slightly worse, and one was equally strong.

Two cases were investigated where the method of introducing the clamping pressure varied. Both cases utilized screws: One case had predrilled holes (screw root diameter), and the other case had clearance holes in the upper two members. The results of these samples are shown in figs. 29 and 30 respectively. Using predrilled holes proved unreliable, with strengths varying significantly, and two samples barely reached any meaningful strength. Investigations of the failure modes showed large sections of the adhesive were poorly bonded. On the other hand, using clearance holes demonstrated performance similar to the benchmark set. The stiffness was roughly equal, and all samples were either almost equally strong or significantly stronger, with one achieving the highest resistance of 80 kN overall.

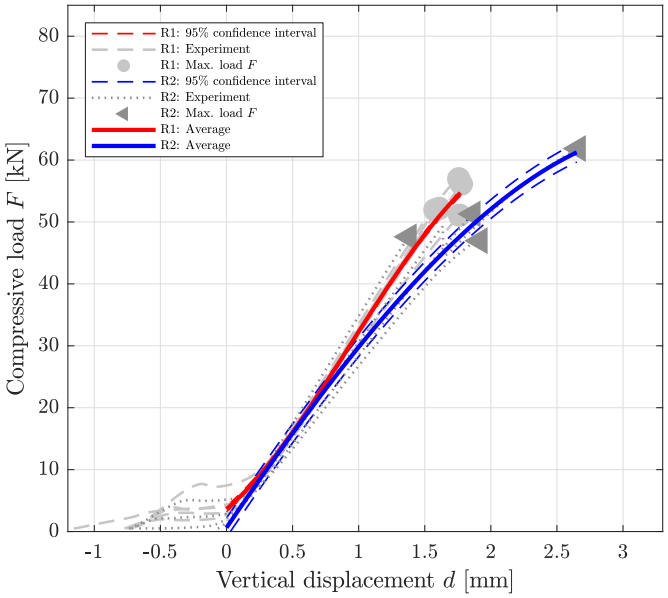

Fig. 27: Load-displacement results of 5% watered-down samples R2 (**blue**) compared to the benchmark samples R1 (**red**).

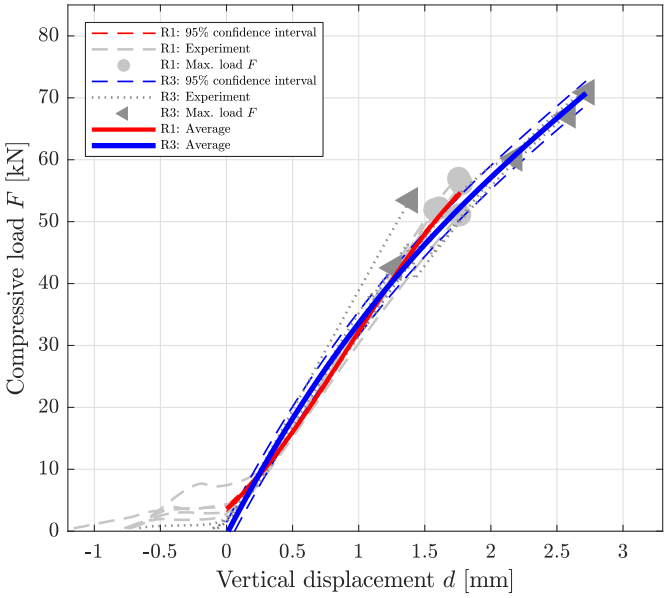

Fig. 28: Load-displacement results of robotic dispensing samples R3 (**blue**) compared to the benchmark samples R1 (**red**).

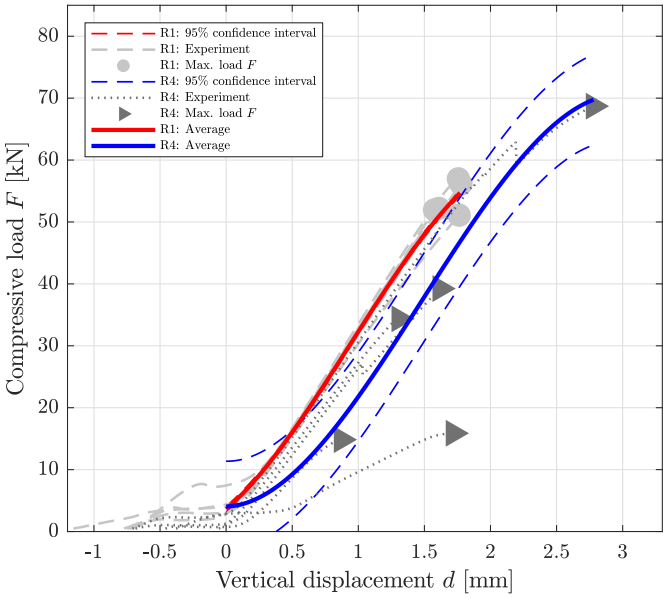

Fig. 29: Load-displacement results of predrilled screw clamping samples R4 (**blue**) compared to the benchmark samples R1 (**red**).

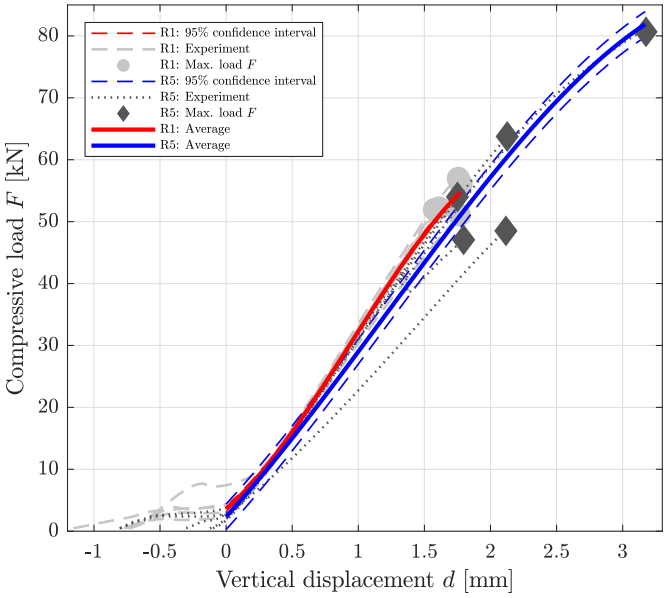

Fig. 30: Load-displacement results of clearance hole screw clamping samples R5 (**blue**) compared to the benchmark samples R1 (**red**).

From literature, it is known that the stress distribution in adhesive bonds is extremely localized. Therefore, simply using the maximum load as an indicator of the strength may not suffice. Consequently, additional analytical and FEM verifications have been performed to assess the stresses in the tested samples. The analytically derived shear and peel stresses along the bond length are shown in figs. 31 and 32 respectively. It can be seen that the shear stresses exhibit large peaks near the adhesive ends, while the majority of the joint remains unstressed. Similarly, the peel stresses peak near the ends, showing a smaller local peak in the opposite direction, with the center of the adhesive remaining unstressed.

The analytical results are compared to a FEM model, of which the stresses are shown in figs. 33 and 34. The maximum stresses found are presented in table I. It can be seen that the shear stresses have similar distributions in both models, with some differences in peak stresses near the ends. The peel stress also shows similar behavior, with a peak stress at the same location and no stress in the center. However, the local peaks indicated by the analytical model are not present in the FEM results.

The maximum stresses occur at the ends of the adhesive, with agreement between the analytical and FEM models. The magnitude of these maximum stresses varies between the two models, with the FEM simulations resulting in more conservative estimates. The shear and peel stresses are higher by 10% and 18%, respectively, at these locations.

The differences between the analytical and FEM results can be attributed to the assumptions made in the analytical model, which is a simplification of real behavior. Moreover, research on adhesive joints is often conducted for thin metallic compositions, as prescribed by ASTM D1002-10. However, this timber joint has significant differences in material properties, ratios, and dimensions compared to this test method, which can explain the different stress patterns observed in the FEM model. Additionally, adhesive stresses are highly sensitive to certain parameters. For example, the thickness of the adhesive layer (assumed to be 0.1 mm) greatly affects the stress magnitudes in the FEM model, whereas the analytical model does not consider the through-thickness stress distribution, which the FEM model does. These sensitivities can explain the differences between the results.

TABLE I: Analytical and ABAQUS maximum stresses in the adhesive layer.

	Max. shear stress τ [N/mm^2]	Max. peel stress σ [N/mm^2]
Analytical	262.83	232.07
ABAQUS	292.31	274.89
Difference	11%	18%

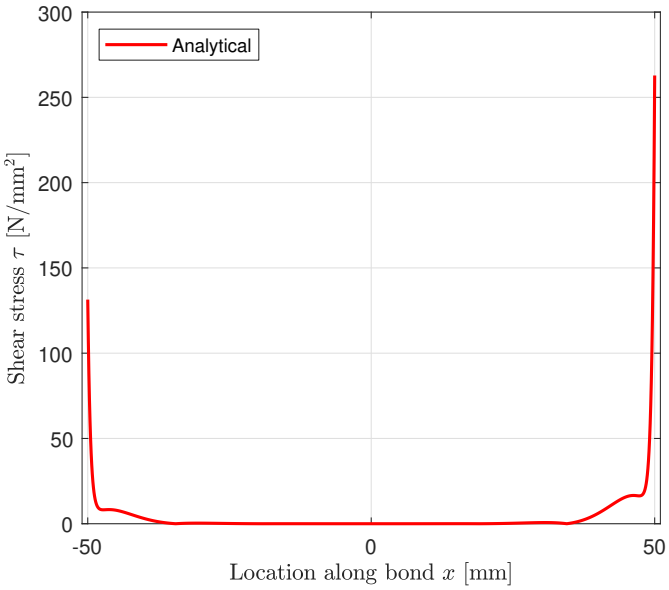

Fig. 31: Analytical shear stresses τ along adhesive.

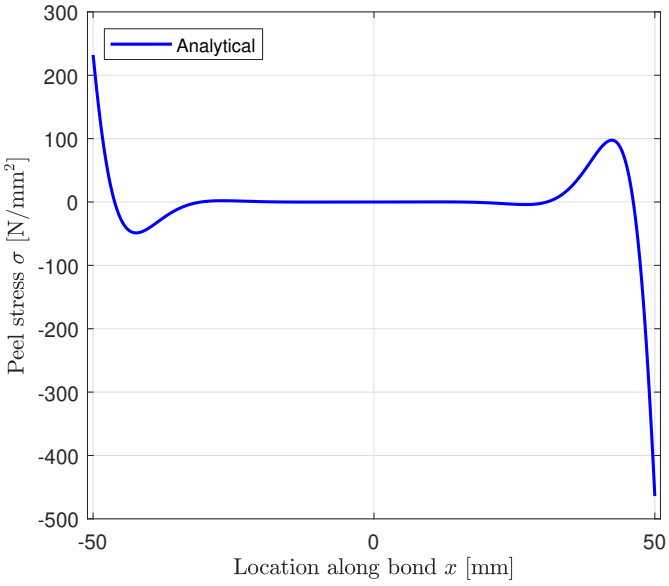

Fig. 32: Analytical peel stresses σ along adhesive.

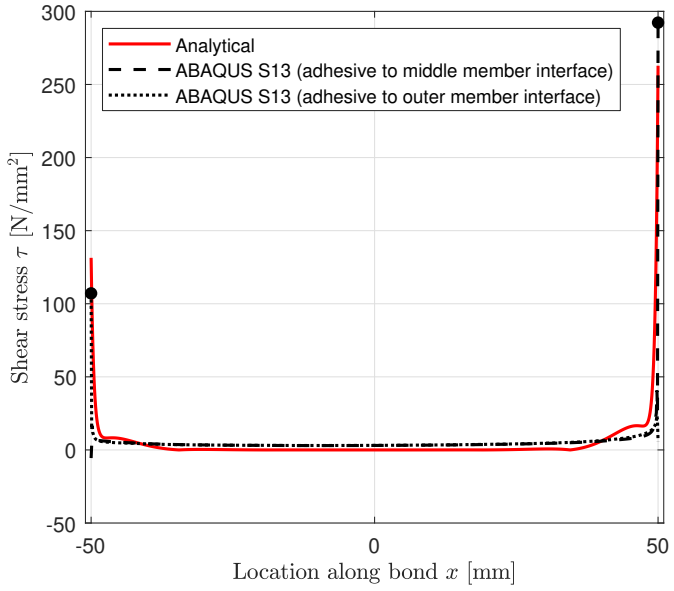

Fig. 33: Analytical and ABAQUS shear stresses τ along adhesive.

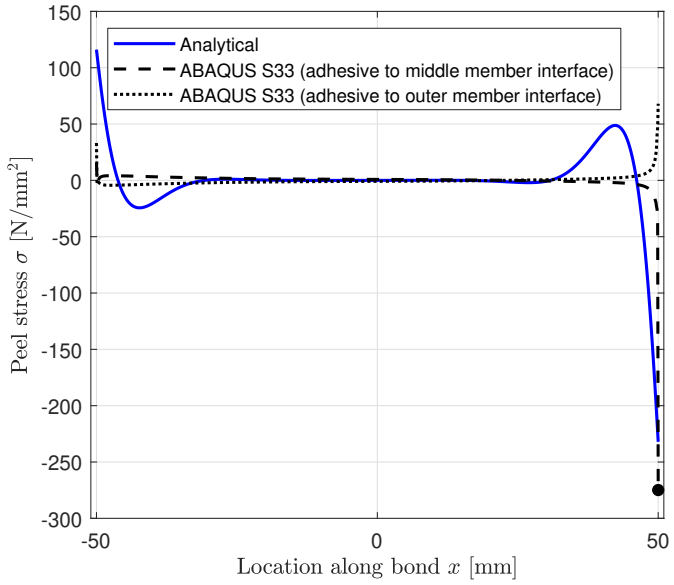

Fig. 34: Analytical and ABAQUS peel stresses σ along adhesive.

V. Discussion

A. Robotic fabrication of adhesive joints

Various parameters of the robotic fabrication process for adhesive joints in timber structures have been examined. The results demonstrate that the robotic process can achieve joints that are equally strong and reliable compared to a traditional adhesive process, provided the proper methods are used. One of the results covered the application of adhesive using a pump in a certain pattern, and then relying on the adhesive spread due to clamping pressure, which had proper distribution over the entire contact area of the joint. This approach is advantageous as it allows for more precise control over the amount of adhesive used. This precision is especially important for minimizing material waste, as very little excess adhesive is pressed out of the joint, while maintaining equal performance.

Traditionally, clamping pressure is introduced using tools such as F-clamps. In a robotic process, this is less desirable because it cannot be easily automated. Therefore, the method of introducing clamping pressure using screws was investigated. This method proved successful, as equal performance was observed in the case of clearance holes. However, there are three important considerations when using screws:

- The type of screw used influences how the members are clamped together. Smooth shanks can guide the screw through the outer members while drilling only into the final member, thereby clamping the entire assembly. In contrast, fully threaded screws do not ensure proper clamping between the members, which can result in the adhesive not bonding correctly at certain points.
- Different types of screws result in different clamping pressures. For the relatively small joints investigated in this research, this was less critical. However, for larger assemblies, it is important to consider the area of effect of the chosen fastener and its clamping pressure. From this, the required minimum number of fasteners must be determined to introduce sufficient clamping pressure.
- The type of adherend preparation greatly influences the effectiveness of the screws. Proper clearance holes guarantee assembly pressure, whereas neglecting this step results in very unreliable joints due to a lack of clamping pressure.

B. Adhesive-fastener hybrid joints

A parallel joint was tested with the fasteners left in place after fabrication. This test was displacement-controlled. During the test, it was observed that once the first adhesive layer failed, the screws kept the assembly together, and the second adhesive layer carried the load. It was noted that the joint's stiffness decreased in this new configuration. The test was not

conducted until failure of the second adhesive layer. However, the conceptual behavior of subsequent failures is illustrated in fig. 35.

With the reduced stiffness, the assembly will experience further loading. As displacement increases, the eccentricity of the assembly also increases, resulting in a further decreasing stiffness. After failure of the second adhesive layer, a significant drop in resistance will be measured, as the screws are considerably weaker and more flexible compared to the adhesive layer. With increasing displacements, the resistance will level out, and the fasteners eventually fail plastically.

Although the fasteners help maintain the assembly's integrity, it is challenging to use them as a proper secondary load path. The adhesive alone provides a very strong shear connection, and to match this strength, significantly larger fasteners would be required. Additionally, the rationale for using a hybrid connection when the strengths are nearly equal remains questionable. The primary consideration might be the increased stiffness of the joint due to the adhesive. However, the adhesive's rigidity compared to the fasteners poses additional challenges. This means that the fasteners will not be activated until the adhesive layers completely fail. When the adhesive fails, the load must be absorbed by the fasteners, which will also involve dynamic effects due to the sudden change, inducing additional stresses. This is particularly important considering that, in reality, the load is force-controlled, not displacement-controlled. This implies that if the first adhesive fails at a certain load, the second adhesive layer will fail immediately as well. For the fasteners to absorb the load, they must be designed to withstand the total load.

C. Adhesive strength prediction

Analytical and FEM models have been developed to assess the stresses in the adhesive samples. Both models indicate that the stress distribution peaks near the ends and zeros out in the middle of the adhesive, which aligns with observations in the literature. This suggests that the overlap length of the adhesive can be chosen economically if designed properly, as large portions of the adhesive are not engaged at failure. Therefore, it is important to carefully determine the required overlap length to avoid making it unnecessarily long.

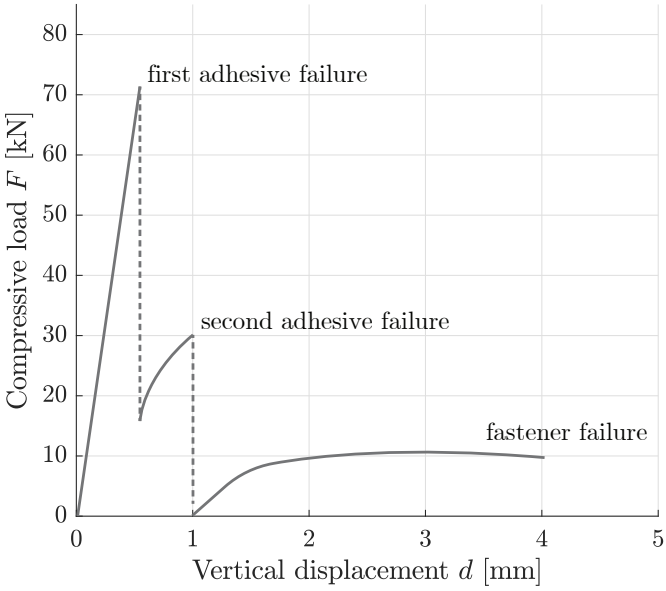

Fig. 35: Conceptual load-displacement behavior of a hybrid connection until failure.

The stress peaks that occur reach relatively high magnitudes, and at failure, explosive failure propagates through the entire bond instantly. These stress peaks can potentially be used to predict the strength of the adhesive bonds. An average shear stress is not suitable for this purpose due to the large inactivated portion of the adhesive, while the stress peaks do dictate the moment of failure. The analytical and FEM models produce varying stress peaks, but literature has shown that the models are sensitive to certain parameters that are currently assumed and difficult to measure accurately, which partly explains the differences. However, more in-depth analysis is required to better understand these differences. A better understanding of the origin of these variations can help develop a more accurate strength prediction criterion.

D. Robotic fabrication process

A successful implementation of the robotic process has been achieved, resulting in a fully automated process capable of fabricating truss elements. However, observations during the process have identified areas for further improvement. The following aspects are recommended to improve:

- **Drilling station:** Currently, the drilling station is stationary, requiring the timber members to be moved to the station. Additionally, the members need to be reoriented multiple times to position the gripper close to the holes.

Future implementations should investigate alternative drilling configurations. For instance, a large, possibly width-adjustable gripper could be designed to properly secure the timber members. Subsequently, a drilling end-effector could drill all holes in one operation, eliminating the need for continuous movement of the timber piece. This approach also opens up possibilities for other end-effectors to perform tasks on the timber members, such as milling or attaching components before assembly.

- **Work object area:** The current setup, with two stationary robots working together, limits the work area and consequently the size of the objects that can be fabricated. It is advisable to expand the robot setup to increase the work area, so that larger objects can be fabricated. This could be achieved by mounting robots on tracks on the ground or suspending them from the ceiling.
- **Weight restrictions:** The robots are relatively small, imposing limitations on the weight and type of elements they can handle. This significantly restricts the structural applicability of the fabricated objects. To address this, utilizing robots with higher handling capacities or creating more powerful grippers would allow for the use of larger and heavier elements.
- **Pick up station:** The existing pick-up station for timber elements relies on the calibration of MDF brackets. Future research should explore the development of smarter algorithms to improve the accuracy and versatility of picking up building blocks. Advanced systems could use cameras to identify objects, their locations, and dimensions, thereby eliminating the need for precise and cumbersome calibration sequences.

VI. Further Research

This research investigated the robotic fabrication of mechanical and adhesive joints and the various parameters involved in this process. Given the scope of this research and its exploration of numerous aspects of the fabrication process, several paths for further study have emerged. The following topics require further investigation:

- **Prediction of stresses in adhesive joints:** Predicting stresses in adhesive joints is challenging for various reasons. While analytical models exist for parallel lap joints, they are sensitive to changes in parameters such as adhesive thickness, which are difficult to measure. Additionally, no closed-form theories exist for adhesive lap joints loaded at an angle, despite their potential frequency (e.g., in trusses). Future research could focus on developing methods to more accurately assess and predict the strength of these joints.
- **Structural behavior of robotically fabricated trusses:** The fabricated truss in this research serves as a validation of the robotic process itself. However, the detailed structural behavior of the entire truss has not been thoroughly investigated. While this study primarily focused on the individual components of the connections and the effects of the robotic process, further research could examine the structural behavior of a robotically fabricated truss composed of adhesive joints.
- **Design of adhesive-screw hybrid connections:** This research explored the use of adhesive-screw hybrid connections. However, designing a safe and reliable hybrid connection requires further attention. Future studies could investigate whether it is possible to create a hybrid connection with specific advantages over using either type of connection alone.
- **Continuous fabrication for longer assemblies:** The robotic fabrication process integrated various steps such as drilling, screwing, and gluing. However, for longer assemblies like the truss, the process had to be discretized. Research could focus on improving the robotic setup to enable the fabrication of continuous members, possibly through the use of external axes using e.g. robots on linear tracks. Other improvements to the efficiency of the robotic setup, such as enhancements to the adhesive pumping system, could also be explored.

By addressing these areas, future research can build on the findings of this study, advancing the field of robotic fabrication in the construction industry.

VII. Conclusion

This research explored the robotic fabrication of shear connections in timber structures using

adhesive, mechanical, or hybrid connections. The robotic setup was developed and validated through a case study involving the fabrication of a truss. Additionally, the research investigated and tested individual aspects of the robotic process to ensure that it performs as reliably as traditional fabrication methods.

The developed robotic system successfully integrated all steps into one workflow: picking and placing, drilling, gluing, and screwing. Experiments comparing these robotic tasks to traditional processes demonstrated that the adhesive joints produced by the robotic system are equally reliable and strong. Therefore, the robotic process can replace manual tasks and automate parts of the fabrication process.

The stresses in the adhesive layers were analyzed using experiments, analytical models, and FEM simulations. The results showed consistent stress distributions, with high stress peaks near the ends of the adhesive and minimal stress in the middle. However, accurately predicting failure loads remains challenging and requires further research.

In summary, this research successfully developed a robotic fabrication system for timber shear joints, such as those in trusses, using either adhesive or mechanical joints. These joints are as strong as those created by conventional methods, making them a suitable replacement and opening up new possibilities for further automation in the AEC industry.

REFERENCES

[1] K. Graser, M. Baur, A. Apolinarska, K. Dörfler, N. Hack, A. Jipa, E. Lloret, T. Sandy, D. Pont, D. Hall, and M. Kohler, "DFAB HOUSE - A Comprehensive Demonstrator of Digital Fabrication in Architecture," pp. 130–139, Apr. 2020.

[2] A. Thoma, A. Adel, M. Helmreich, T. Wehrle, F. Gramazio, and M. Kohler, "Robotic Fabrication of Bespoke Timber Frame Modules," in *Robotic Fabrication in Architecture, Art and Design 2018* (J. Willmann, P. Block, M. Hutter, K. Byrne, and T. Schork, eds.), (Cham), pp. 447–458, Springer International Publishing, 2019.

[3] H. J. Wagner, M. Alvarez, A. Groenewolt, and A. Menges, "Towards digital automation flexibility in large-scale timber construction: integrative robotic prefabrication and co-design of the BUGA Wood Pavilion," *Construction Robotics*, vol. 4, pp. 187–204, Dec. 2020.

[4] Gramazio Kohler Research, "Digital assembly of a complex roof structure," 2016.

[5] K. Johansen, "Theory of timber connections," *Publications of International Association for Bridge and Structural Engineering*, no. 9, pp. 249–262, 1949.

[6] R. Kliger, M. Johansson, R. Crocetti, M. Annika, H. Lidelöw, B. Norlin, and A. Pousette, *Design of Timber Structures - Structural Aspects of Timber Construction*, vol. 1. Stockholm: Swedish Forest Industries Federation, 3 ed., 2022.

[7] M. Domínguez, J. G. Fueyo, A. Villarino, and N. Anton, "Structural Timber Connections with Dowel-Type Fasteners and Nut-Washer Fixings: Mechanical Characterization and Contribution to the Rope Effect," *Materials*, vol. 15, p. 242, Dec. 2021.

[8] H. J. Blaß and C. Sandhaas, *Timber Engineering - Principles for Design*. 2017.

[9] G. Lantos, "Load Distribution of a Row of Fasteners Subjected to Lateral Load," *Wood Science*, vol. 1, no. 3, pp. 129–136, 1969.